*International Journal of Advanced Technology and Engineering Exploration, Vol 10(98)*
*ISSN (Print): 2394-5443 ISSN (Online): 2394-7454*
*http://dx.doi.org/10.19101/IJATEE.2021.874950*

Research Article

# Analysis of hardness for dissimilar stainless-steel joint by mathematical modelling

**Deeksha Narwariya[1*] and Aditya Kumar Rathi[2]**
Research Scholar, Department of Mechanical Engineering, MPAE Division, Netaji Subhas University of Technology, India[1]
Associate Professor, Department of Mechanical Engineering, MPAE Division, Netaji Subhas University of Technology[2]

Received: 15-July-2021; Revised: 14-January-2023; Accepted: 17-January-2023


## Abstract
***Gas tungsten arc welding (GTAW) is very popular globally as it is capable of doing similar and dissimilar material welding. Most commonly steel and aluminium of different grades are joined using this process. In this research work, two unalike grades of stainless steel i.e., 304 and 316 were welded together with different combination of parameters. An attempt was made to find out the effect on the surface hardness of the joint. The parameters under consideration were current, welding speed and torch angle, having two limits, maximum limit (+1) and lower limit (-1). A mathematical model was developed between input parameters and the responses such as hardness was analyzed by using the factorial approach. The result of the analysis shows that increase in current and welding speed decreases the hardness whereas an increase in torch angle increases the surface hardness. Hardness is maximum at the weld zone of two dissimilar metals and minimum at the heat affected zone.***

## Keywords
***Stainless steels, GTAW, Surface hardness, Input parameters, ANOVA.***

## 1.Introduction
There are certain concerns when we need that a joint must be of different metal compositions. This also applies to higher temperature applications or of wear situations. In such situations and other related problems, one has to think of dissimilar metal joints. Two different grades of stainless steel with different combination of the input parameter can be joined together. The combination of the different parameter leads to obtain desired results. These input parameters can be current, table speed and torch angle, variation in these parameters can cause alteration in mechanical properties. These changes are also responsible for the change in stability of arc, melting and deposition rate [1]. For welding dissimilar metals, the following four things we have to keep in mind, melting point of metals, coefficients of their thermal expansion, electrochemical difference and solubility of each metal [2]. If fusion welding is used, melting point plays an important role.

*Author for correspondence

Similarly, the coefficient of thermal expansion can create excessive strain in the weld zone if there is more difference in it. Electrochemical difference can relate to corrosion in the inter metallic zone [3].

Metals that fit closer to electrochemical scale can provide simple welding process than those that are far apart. Solubility of each metal is another problem which is to be taken care [4]. If these are not interpolable with each other than third metal is used as a filler metal which is soluble with these metals [5]. The process available for joining dissimilar metals are fusion and nonfusion welding along with low dilution welding. The last two methods are used for high output and special welding application [6]. Most commonly used process for dissimilar metal welding (DMW) in power and process industries are fusion welding [4].

The purpose of the paper was to study the surface hardness of welded joints. The combination of these materials will make a joint very useful for certain applications because these can sustain the extreme

environmental condition for corrosion. These are easily weldable at the given thickness so the problem of solubility and melting point can be dealt easily with such type of dissimilar fusion welding. Some of the important applications are heat exchangers, pipelines, pressure vessels, flanges and fittings. Effect of welding parameters on the hardness an be easily seen in this work.

This paper is organized and explored in the following sections. Literature discussion in section 2. Methods have been explored in section 3. Results investigation and the discussion has been presented in section 4. The concluding remark has been elaborated in section 5.

## 2.Literature review

The metallurgical and mechanical characterization of dissimilar joints between low carbon steel and stainless steel was made by laser autogenous welding. The results demonstrate that the affirmative difference in yield between the weld metal and the base materials assist the joint from being plastically deformed [7]. Another researcher presented in his paper that deeper qualitative analysis of the welding procedure's influences the fracture toughness of the High strength low alloy (HSLA) steel welded by manual metal arc (MMA) and metal active gas (MAG) process [8]. High temperature during welding has an affirmative outcome on the micro-structure and it was observed that material failure occurred in the base material near the heat affected zone (HAZ) while manufacturing American iron and steel institute (AISI) 316L stainless steel tubes with Selective laser melting (SLM) technology [9]. Hydrogen analysis and scanning electron microscopy (SEM) were conducted to find the effect of charging time on the hydrogen concentration and surface Morphology of hydrogen exposed 316L stainless steel welded joints at ambient and cryogenic temperature. The result shows that vulnerability to hydrogen decreased the absorbed energy and ductility of 316L stainless steel at all tested temperatures but not much difference was found among the pre-charging times [10]. Gas tungsten arc welding (GTAW) can be more widely used in aerospace components and food processing units by welding sheets and pipes [11]. Stainless steel 316 is mostly used in Thermal power plants, its study for temperature time precipitation (TTP), when it is used in high temperature applications [12]. Underwater wet welding of 317L stainless steel with nickel based tubular wire shows that fully austenitic weld metal without cracks and pores with nickel-based filler wire can be achieved as observed in the micro-structure analysis [13]. Dissimilar welding was done on small thick plates with different fluxes on Tungsten inert gas (TIG) to micro-structure examination with the best outcome in case of $TiO_2$ ingredients [14]. Similarly, a dissimilar welding was performed on unlike grades of steel where related parameters were optimized by Taguchi analysis on a tensile test specimen [15]. A dissimilar weldment between P91 and American iron and steel institute (AISI) 316L austenitic steel fabricated by activated TIG welding was performed on 8 mm thick plates using a single pass with pre-coated mixture of metallic oxides the result shows that elimination of hot cracking in the joint compared with conventional methods is very helpful [16]. The mechanical and micro-structural properties can be enhanced by using filler material such as 309L when joining similar grades of stainless steel by TIG welding, the best result is obtained by 120 A current [17]. Influence of welding parameters such as welding current and welding speed was carried out to find the strength of joint welded by TIG welding in between low carbon steel and aluminium alloy AA1050 the result shows that at an optimized value of strength with the help of Taguchi analysis can be achieved [18]. SS 304 and carbon steel welded together with TIG and A-TIG process and it was found that A-TIG welded joint has better joint efficiency and mechanical properties as compared to TIG welded joints [19]. Optimization of process parameters was done on naval steel to get the maximum depth of penetration by using GTAW process. Response surface methodology (RSM) D-optimal method and Taguchi optimization techniques were compared, and it showed that RSM result is better than Taguchi analysis for better penetration [20]. Artificial neural network (ANN) was used for simulation, and genetic algorithm (GA) was used to optimize the process parameters such as welding current, welding speed, nozzle deflection distance, travel angle and wire feed frequency for GTAW process on AISI 1020 steel blank material with two tubular wires [21]. A TIG welding process was used to study the effect of welding speed and welding current on welding of mild steel plates it was concluded that current can be increased up to 110 A for 6 mm thick plates to get the best hardness result. A further increase in current will reduce the hardness [22]. Shielded metal arc welding (SMAW) was performed on A 36 carbon steel welded joint to study the effect of welding current on the micro structure and hardness of the joint. Results indicate that the higher current reduces strength and hardness [23]. A dissimilar joint of AA 6063 with AA 7075 was made

with the help of friction stir welding (FSW) process to study the effect of spindle speed and welding speed, the result shows that increasing the spindle speed and decreasing the welding speed gave the best result of tensile strength [24]. A study of metal inert gas (MIG) welding process carried out on carbon steel plates says that the hardness of the joint increases with the decrease in welding speed and increase in welding current [25]. The effect of gas flow rate on welded stainless-steel alloy SS-202 joint was studied and the result shows that at a low gas flow rate high tensile strength and low ductility were achieved whereas at high welding speeds high tendency of welding defects and improper penetration takes place [26].

As per the latest research, software simulation is also useful to study the dissimilar metal welded plates of 20/0Cr18Ni9 by finite element analysis the result shows that residual stress of each model is significantly reduced. The stress reduction of 20 steel side is significantly larger than on the 0Cr18Ni9 side and deformation was smaller in each case after the heat treatment [27]. Dissimilar metal joining investigation of AISI 316L-Alloy800 by activated TIG. (A-TIG) shows that joint has a decent combination of tensile strength and impact toughness [28]. The propeller shaft made by joining steel ST41 and 316L stainless steel with a variety of electrode in SMAW process the result of the analysis shows that the tensile strength of the base material increases and use of E6013 electrode has lower corrosion resistance [29]. Micro-structure and corrosion behavior of copper and 316L stainless steel welded joints on an electrolytic copper cathode plate was investigated. Clear phase separation was noted in the weld metal with the γ- and ε-Cu phase dominating the Fe-rich and Cu-rich zones, respectively [30]. A dissimilar joint of aluminium alloy and commercially used copper alloy by friction stir spot welding (FSSW) process shows that the optimized result of welding parameters can be obtained by the weighted aggregated sum product assessment coupled with grey wolf optimization method and pin length is the most significant factor [31]. Mechanical properties and crack propagation behavior was investigated of pressurized water reactor for cladding layer material 304L and SA508 the result indicated that the strength value at the fusion boundary is largest and yield strength reaches at 689 Mpa [32]. As per the literature review, one can say that a lot of work already done on the dissimilar weld joint but to the best knowledge, dissimilar TIG joint of SS 304 and SS 316 of 2 mm is still remains. So, an effort was made on dissimilar grades of SS 304 and SS 316 steel on the TIG welding by considering the combination of different level of input parameters.

## 3.Methods

The following path was followed while carrying out the fact-finding work.

1. Selection of material
2. Problem with welding of stainless steel
3. Recognizing the input parameters
4. Establishment of a design matrix
5. Experimentation for the responses
6. Generation of the mathematical model
7. Analysing the graphs and plots

### 3.1Experimental setup

In the present study, TIG welding machine of flat V-I (voltage and current) characteristics was used. For sample preparation shielded gas as argon was used to weld two different grades of steel plates with non consumable electrode of 2.5 mm diameter. The sample dimensions were kept as 150 mm square and 2 mm thick. The Rockwell hardness test is the most widely used it has 3 type of scales A, B, C. B scale was used in this case according to the data book as maximum hardness of SS 304 is 70 Rockwell hardness at B scale (HRB) and SS 316 is 78 HRB. Experimental setup is shown in *Figure 1(a)*, consist of a welding torch and the platform to weld the specimen. Welding of dissimilar steel 2 mm plates in process is shown *Figure 1(b)*. Fixing of plates to make a butt joint is shown in *Figure 1(c)* before the welding. Plates are butted against each other and a clamping device will hold the plates together. The joint after the welding operation is shown in *Figure 1(d)* before making the specimen for other testing processes.

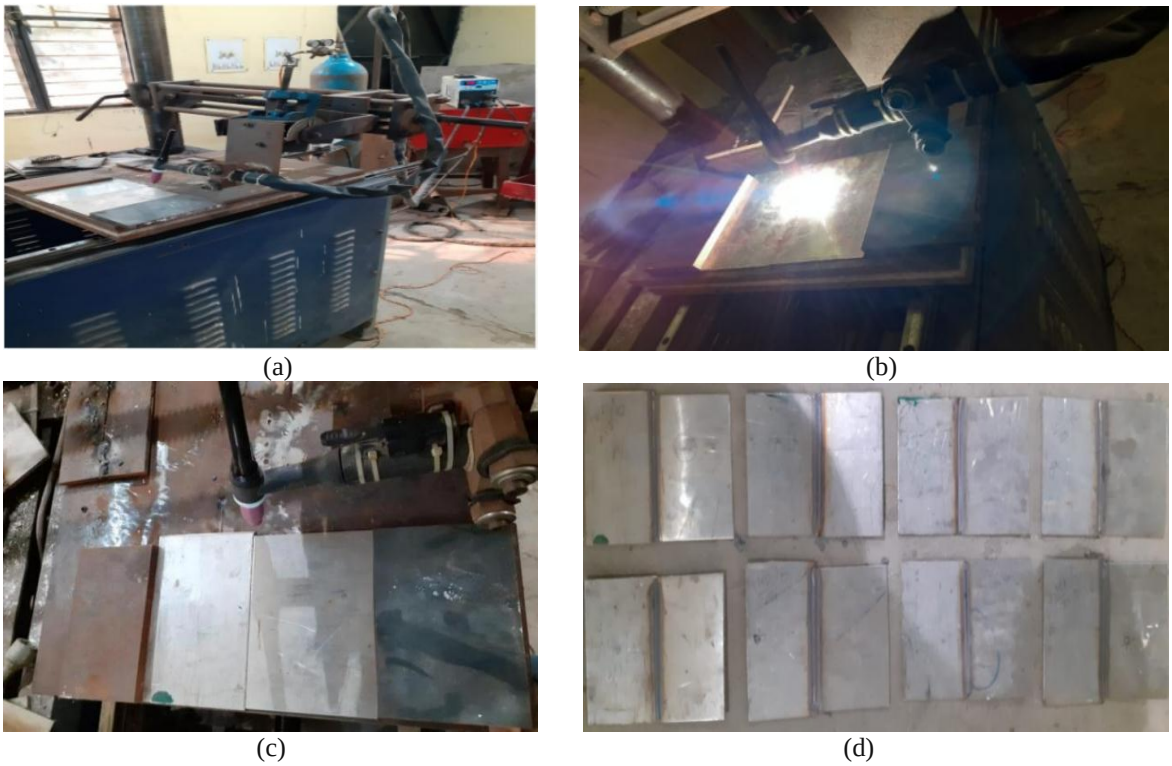

(a) (b)

(c) (d)

**Figure 1** (a) TIG welding setup (b) welding of specimen (c) SS304 and SS316 specimen (d) welded specimen

### 3.2Selection of material

Stainless steels are a ferrous alloy that contains chromium which protects the ferrous content from rusting and also enhance heat resistant property. Stainless steel being resistant to corrosion, can be used in many applications. The important point is that it can be easily shaped into plates, sheets, bars and tubes. Important applications are heavy industries, construction material and surgical equipments. It also does not require any surface treatment mostly used in kitchen appliances and food processing units. So, AISI 304 and AISI 316 were selected for the study purpose. The chemical composition of these two have been discussed.

AISI 304 which is Chromium-Nickel based steel, mostly used as 300 series stainless steel, it has superior forming and welding attributes. The cautiously controlled investigation of 304 made it to be deep drawn more seriously than types 301 and 302 without in-between heat demulcent. AISI 304 also has prominent welding attributes. In a gently corrosive environment, no post-weld annealing required to regenerate the superior performance of this grade. Chemical composition of SS304 is given in *Table 1*.

**Table 1** Composition of SS304

| S. No. | Elements | Weight (%) |
|---|---|---|
| 1 | Carbon | 0.060 |
| 2 | Manganese | 0.86 |
| 3 | Silicon | 0.031 |
| 4 | Chromium | 18.35 |
| 5 | Nickel | 8.20 |
| 6 | Phosphorus | 0.031 |
| 7 | Sulphur | 0.01 |

By adding 2.5% molybdenum in 316/316L an austenitic steel increased ace corrosion resistance of this type 304 grade. 316L has reinforced indentation corrosion opposition and has superior mechanical phenomenon to sulphates, phosphates and others. 316/316L has better resistance than standard 18/8 types of salt water, acids, chlorides, bromides and iodides. Its chemical mixture is given in *Table 2*.

**Table 2** Components of SS316

| S. No. | Elements | Weight (%) |
|---|---|---|
| 1 | Carbon | 0.04 |
| 2 | Manganese | 1.6 |
| 3 | Silicon | 0.05 |
| 4 | Chromium | 19 |
| 5 | Nickel | 12.5 |
| 6 | Phosphorus | 0.03 |
| 7 | Sulphur | 0.03 |

### 3.3Problem in TIG welding of stainless steel

Steel is mainly used because of its anti-corrosion property. Chromium and carbon adversely effected in the form of corrosion called weld decay or inter-crystalline corrosion. During welding nearby carbon dissolves with chromium and then on cooling precipitate as chromium carbide on the grain boundary hence, it is going to lose its corrosion resistance property. There are so many techniques. The most obvious are either reduce carbon content or add some alloying element which can react and avoid the formation of chromium carbide. Higher expansion in the heat affected zone results in increased thermal stresses hence more distortion. For welding of thin sheet where more dimensional tolerance is required, which can be achieved by use of accelerated cooling process like copper chills or freezing gas. That makes processing more tedious and costly. TIG welding of stainless steel is carried out within the inert gas atmosphere otherwise chromium present in the ferrous alloy reacts and form a compound. Generally, argon gas is used and sometimes nitrogen can also be used, but there is the risk of hot cracking in the case of nitrogen. Stress corrosion cracking in fabrication industries, is the other problem. It may occur due to halides or strong alkali solution. Cracking occurs at high stress region. Stresses in the region near by weld reaches to yield point of metal and cracking propagate rapidly. Stress relieving process at the temperature 700 to 900˚C has to be used to avoid this failure.

### 3.4Important process factor

On the ground of literature survey, test runs were performed, it showed that weld properties are related to current, welding speed and torch angle very much. Where as no significant effect was seen due to gas flow rate. Keeping in mind it was kept constant 15 l/min throughout the experiment. Once the important input variable was found, their working extent was ascertained by performing trial runs. Such as, increasing one parameter over its range and keeping others as constant by checking the quality of weld in reachable range as far as weld bead and any surface fault is concerned. All the process parameters are given in *Table 3.*

### 3.5Formation of a design matrix

Using MINITAB software, the design formula was prepared. Two levels of welding current were chosen as 120 and 140 Amp. Welding speed levels was chosen as 25 and 35 cm/min. Torch angel was varied from 0-45˚. Further welding was performed according to the design matrix, whereas weld run was performed in different combination of input parameters. The design matrix in coded form is shown in *Table 4.* +1 indicates higher level and -1 indicates lower level. Process flow diagram is shown in *Figure 2*.

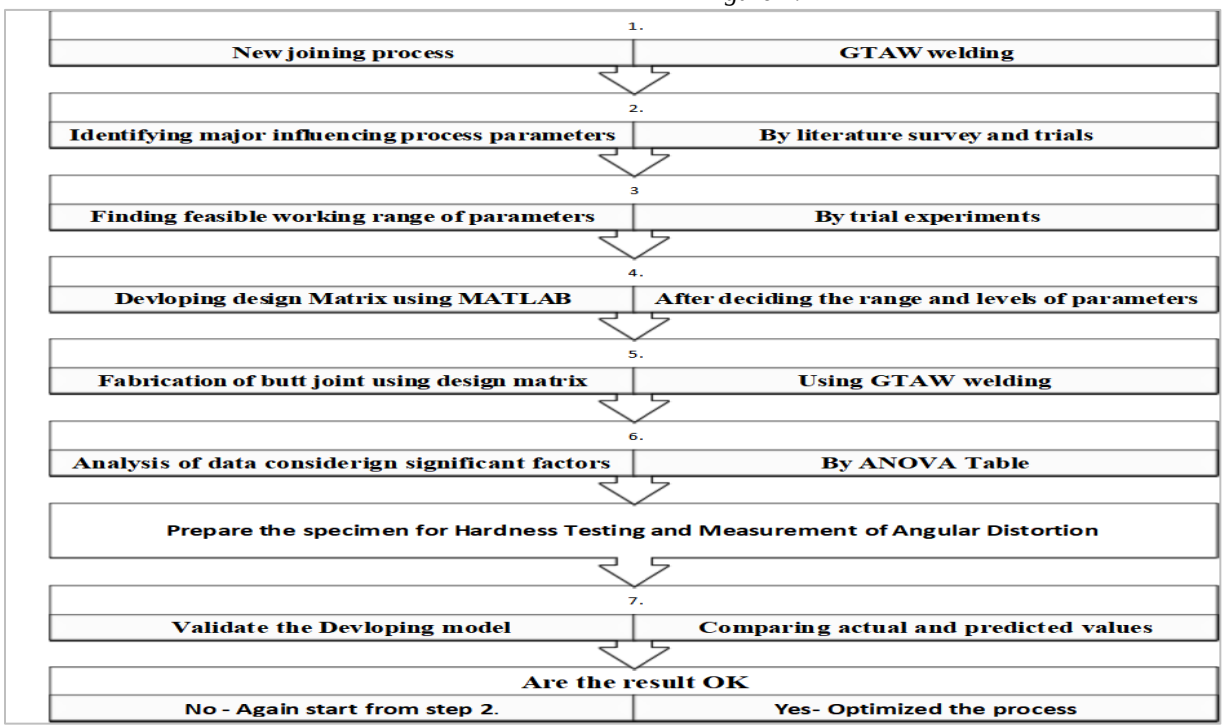


**Figure 2** Process flow diagram

**Table 3** Important factors

| S. No. | Parameters | Parameter limits |
|---|---|---|
| 1 | Welding current | 120 - 140 Amp |
| 2 | Welding speed | 25 - 35 cm/min |
| 3 | Torch angle | 0 - 45 ˚ |
| 4 | Voltage | 15 V |
| 5 | Tungsten electrode diameter | 2.5 mm |
| 6 | Inert gas | Argon |
| 7 | Nozzle to tip distance | 2mm |

**Table 4** Design matrix

| S. No. | Current | Welding speed | Torch angle |
|---|---|---|---|
| 1 | -1 | +1 | -1 |
| 2 | +1 | -1 | +1 |
| 3 | -1 | -1 | +1 |
| 4 | -1 | -1 | -1 |
| 5 | +1 | +1 | +1 |
| 6 | +1 | -1 | -1 |
| 7 | -1 | +1 | +1 |
| 8 | +1 | +1 | -1 |

# 4.Results

## 4.1Experimentation for the response: (Hardness)

The surface hardness was measured using a Rockwell hardness testing machine with diamond indenter. Initially, a load of 10 kgf was applied so that there is good connect between work piece and diamond shaped indenter. After that a primary load of 150 kgf was applied as per the workpiece material. Waiting time of 60 sec was set so that any fluctuation in dial gauge can be minimized. Now release the load and note down the scale reading. It was planned to take 3 readings, one in the weld area and two on the both sides of the weld bead. The machine used to take the Brinell hardness number (BHN) of the specimens at three different points is shown in *Figure 3*. Measured hardness of different specimens is shown in *Table 5*.


**Figure 3** Measurement of the hardness using the Rockwell hardness testing machine

**Table 5** Measurement of surface hardness

| S. No. | Current (Amp) | Welding speed (cm/min) | Torch angle (degree) | H1 | H2 | H3 |
|---|---|---|---|---|---|---|
| 1 | 140 | 35 | 0 | 47 | 65 | 53 |
| 2 | 120 | 25 | 45 | 80 | 98 | 90 |
| 3 | 140 | 35 | 45 | 54 | 70 | 62 |
| 4 | 140 | 25 | 0 | 69 | 88 | 81 |
| 5 | 120 | 25 | 0 | 72 | 89 | 83 |
| 6 | 120 | 35 | 0 | 63 | 86 | 75 |
| 7 | 120 | 35 | 45 | 76 | 95 | 88 |
| 8 | 140 | 25 | 45 | 74 | 90 | 85 |

## 4.2Generation of the mathematical model

After measuring the surface hardness, a mathematical relation was developed between input parameters and the responses. Hardness was measured at three points, one of the weld zones represented as H2 and other two at the HAZ on the both regions of the weld.

H1 represents the hardness of the heat affected zone on the SS 304 while H3 represents the same on the SS 316 side. Analysis of variance (ANOVA) analysis of hardness at point H1 is shown in *Table 6.* Analysis of the result shows that regression model is significant as its P-value is 0.018. The most significant factor is interaction of current and speed which is having a P-value as 0.018. After that next significant factor is speed having a P-value of 0.022. The model summary says that R-square value is 0.999 shows that 99.9 % variation is shown by the independent variables. The value of R-square (adjusted) and R-square (predicted) is in close agreement.

**Table 6** ANOVA for H1

| Source | Degree of freedom (DF) | Adjusted sum of squares (Adj SS) | Adjusted mean squares (AdjMS) | F-Value | P-Value |
|---|---|---|---|---|---|
| Regression | 6 | 1748.75 | 291.458 | 2331.6 | 0.016 |
| Current | 1 | 222.37 | 222.368 | 1778.9 | 0.015 |
| Speed | 1 | 276.48 | 276.48 | 2211.8 | 0.014 |
| TA | 1 | 22.85 | 22.837 | 182.70 | 0.047 |
| current×speed | 1 | 351.12 | 351.125 | 2809.0 | 0.012 |
| current×TA | 1 | 28.12 | 28.125 | 225.00 | 0.042 |
| speed×TA | 1 | 3.13 | 3.125 | 25.00 | 0.126 |
| Error | 1 | 0.13 | 0.125 | - | - |
| Total | 7 | 1748.88 | - | - | - |

S=0.353553, R-square=99.99%, R-square (adjusted)= 99.94%, R-square(predicted)= 99.43%

H1=-147.7+ 2.0250 current+ 9.575 speed + 1.0444 TA - 0.08750 current × speed- 0.007222 current × TA + 0.00333 speed × TA (1)

H2=-287.8+ 3.2500 current+ 15.375 speed + 1.0778 TA - 0.13250 current × speed - 0.008333 current × TA + 0.0056 speed × TA (2)

ANOVA analysis of hardness at point H2 is shown in *Table 7*. Analysis of the result shows that regression model is significant as its P-value is 0.016. The most significant factor is interaction of current and speed which is having a P-value as 0.012. After that next significant factor is speed having a P-value of 0. 014. The regression equation for the model of hardness at point H1 is shown by Equation 1. The model summary says that R-square value is 0.999 shows that 99.9 % variation is shown by the independent variables. The value of R-square (adjusted) and R-square (predicted) is in close agreement.

ANOVA analysis of hardness at point H3 is shown in *Table 8*. Analysis of the result shows that regression model is significant as its P-value is 0.015. The most significant factor is interaction of Current and speed which is having a P-value as 0.013. After that next significant factor is speed with a P-value of 0.015. The Regression equation for the model of Hardness at point H2 is shown by equation 2. The model summary says that R-square value is 0.999 shows that 99.9 % variation is shown by the independent variables. R-square (adjusted) and R-square (predicted) is in close agreement.

**Table 7** ANOVA for H2

| Source | DF | Adj SS | Adj MS | F-Value | P-Value |
|---|---|---|---|---|---|
| Regression | 6 | 1406.75 | 234.458 | 1875.67 | 0.018 |
| Current | 1 | 86.33 | 86.329 | 690.63 | 0.024 |
| Speed | 1 | 107.23 | 107.229 | 857.83 | 0.022 |
| TA | 1 | 21.45 | 21.447 | 171.57 | 0.049 |
| current*speed | 1 | 153.12 | 153.125 | 1225.00 | 0.018 |
| current*TA | 1 | 21.12 | 21.125 | 169.00 | 0.049 |
| speed*TA | 1 | 1.13 | 1.125 | 9.00 | 0.205 |
| Error | 1 | 0.13 | 0.125 | - | - |
| Total | 7 | 1406.88 | - | - | - |

S= 0.35355, R-square=99.99%, R-square (adjusted)=99.93%, R-square (predicted)=99.59%

**Table 8** ANOVA for H3

| Source | DF | Adj SS | Adj MS | F-Value | P-Value |
|---|---|---|---|---|---|
| Regression | 6 | 1934.75 | 322.458 | 2579.67 | 0.015 |
| current | 1 | 192.64 | 192.645 | 1541.16 | 0.016 |

| Source | DF | Adj SS | Adj MS | F-Value | P-Value |
|---|---|---|---|---|---|
| speed | 1 | 217.12 | 217.124 | 1736.99 | 0.015 |
| TA | 1 | 17.54 | 17.536 | 140.29 | 0.054 |
| current×speed | 1 | 300.12 | 300.125 | 2401.00 | 0.013 |
| current×TA | 1 | 28.12 | 28.125 | 225.00 | 0.042 |
| speed×TA | 1 | 15.13 | 15.125 | 121.00 | 0.058 |
| Error | 1 | 0.12 | 0.125 | | |
| Total | 7 | 1934.88 | | | |

S=0.333, R-square=0.999, R-square (adjusted)=99.9%, R-square(predicted)= 99.44%

H3=-252.2 + 3.0250 current + 13.625 speed + 0.9444 TA- 0.12250 current × speed- 0.008333 current × TA + 0.01222 speed × TA (3)

The regression equation for the model of hardness at point H3 is shown by Equation 3.

## 5.Discussion

ANOVA of the formulated model, has P-value, less than 0.05 that signifies the model. The most important factor is the interaction of welding current with welding speed and then the angle of the torch. Secondly, the high numerical quantity of R square and adjusted R-square also propose the satisfactoriness of the formulated exemplary.

### 5.1Line plot for hardness along the welded specimen

From the line plot it is observed that hardness of SS 304 is less than SS 316. H1 is the hardest on the heat affected zone of material SS 304 and H3 is the hardness of heat affected zone of material SS 316. On the welded specimen, hardness first increases, then start to decrease. Hardness is maximum at the weld joint as the metal solidifies, it recrystallizes itself into fine grain which makes it hard and brittle in nature.

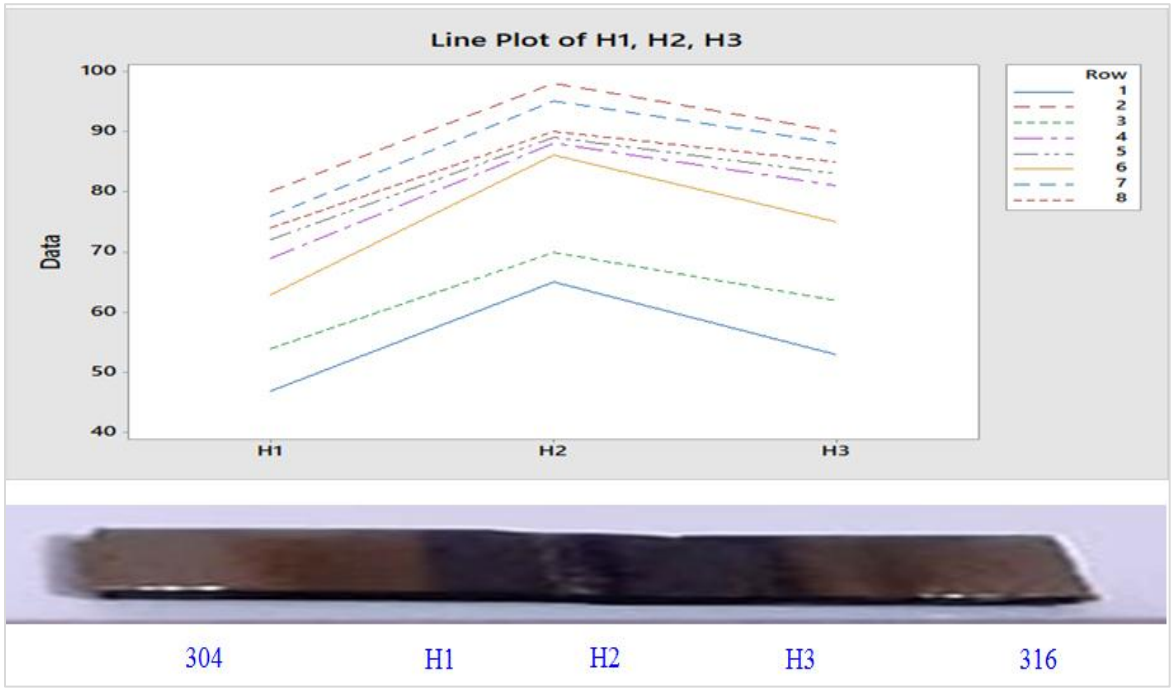


**Figure 4** Line plot of hardness along welded specimen for different weld runs

Whereas when move towards the base metal grains gets coarser again resulting decrease in hardness. The line plot of the hardness is shown in *Figure 4*. It is clear from this that the hardness at base metal is less than the weld metal. Position of taking the hardness value from the specimen is also shown in *Figure 4.* Maximum hardness is observed at the welding current of 120 Amp, 25 cm/min welding speed and 45 $^0$ Torch angle. Minimum hardness is observed at 140 Amp current, 35 cm/min welding speed and $0^0$ torch angle.

## 5.2Main effect plot of hardness with the input parameters

### 5.2.1Hardness versus current

An increase in current, hardness starts to decrease because increases in current causes more heat supplied to the base metal which promotes the austenite micro-structure formation that enhance the strength of the metal and decreases the hardness. The result is shown in *Figure 5 (a).* Hardness plays an important role for mechanical properties of material, if hardness is more material becomes brittle and it cannot be used in many applications. It is also justified by [24, 25] that the value of current can be increased up to a level after that it will decrease the hardness in the TIG welding process.

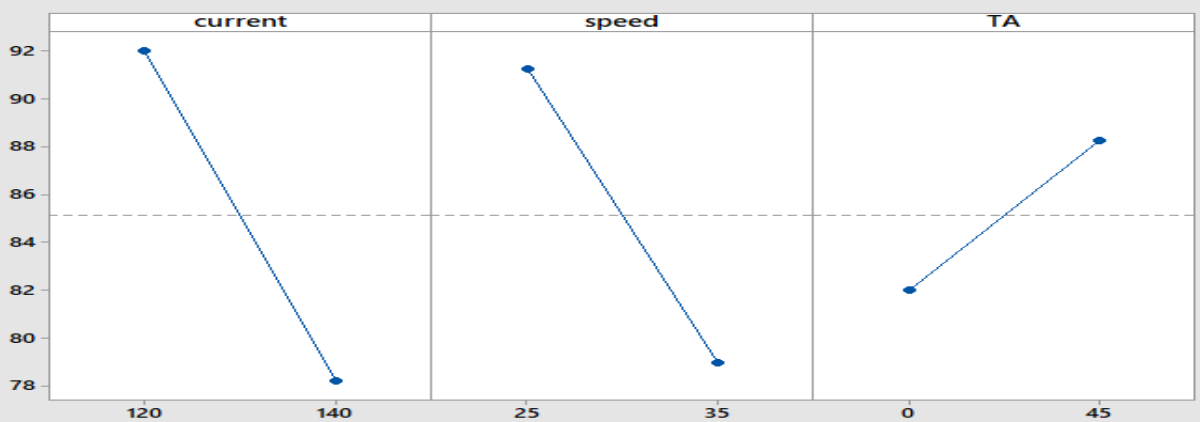


(a) (b) (c)

**Figure 5** Main effect plot of input parameters with hardness

### 5.2.2Hardness versus speed

An increase in the speed, decreases hardness. The reason is heat input per unit area, per unit time decreases which results in thermal stresses generation, hence less grain boundary and less hardness. The result is shown in *Figure 5 (b).* Effect of welding speed is explained in the FSW by [26] shows that it has a mixed effect on hardness of the weld zone. In the MIG welding process, hardness increases with the decrease in welding speed. Our results are also in the same line. Mixed effect is also observed by [27] on hardness in MIG welding process for stainless steel alloy-202.

### 5.2.3Hardness versus torch angle

As the torch angle increases the spread of flame increases the heat affected zone also increases. More stresses causing more grain boundary and make finer grains and ultimately increases the hardness of the metal. The result is shown in *Figure 5(c).* The angle of the torch was taken as $0^0$ and $45^0$. Heat input is directly related to the torch angle as we increase the torch angle the heat input will spread over a large area and penetration will decrease.

## 5.3The combined effect of input parameters on the hardness

### 5.3.1Hardness vs. speed and current

ANOVA *Table 6, 7, 8* exhibits that interaction of speed and current is significant for all the three cases. *Figure 6* represents the 3D plots of hardness with current and speed. It shows that the decrease in current and speed both will increase the hardness. The maximum hardness can be achieved at current of 120 Amp and a speed of 25 cm/min. The maximum value of hardness achieved as BHN of approximate as 78. The pattern of the plot is also a straight line that indicates that hardness is linearly related to current and speed.

### 5.3.2Hardness vs. Torch angle and current

ANOVA *Table 6, 7, 8* exhibits that interaction of Torch angle and current is significant for all the three cases. *Figure 7* represents the 3D plots of hardness with current and Torch angle. It shows that the decrease in current and increase in Torch angle will increase the hardness of the joint. The maximum hardness can be achieved at current of 120 Amp and Torch angle of $45^0$. The maximum value of hardness achieved as BHN of approximate as 76 to 78. The lower value of current and minimum torch angle gave higher hardness.

### 5.3.3Hardness vs. Torch angle and speed

ANOVA *Table 6, 7, 8* exhibits that interaction of Torch angle and speed is the most significant factor for the first two cases, whereas in the third case it is also significant with P-value as 0.048. *Figure 8* represents the 3D plots of hardness with speed and Torch angle. It shows that the addition in Torch angle will increase the hardness whereas speed is almost

constant. The maximum hardness can be achieved at speed 25cm/min and Torch angle of $45^0$. The Maximum value of hardness achieved as BHN of approximate 80. A complete list of abbreviations is shown in *Appendix I.*

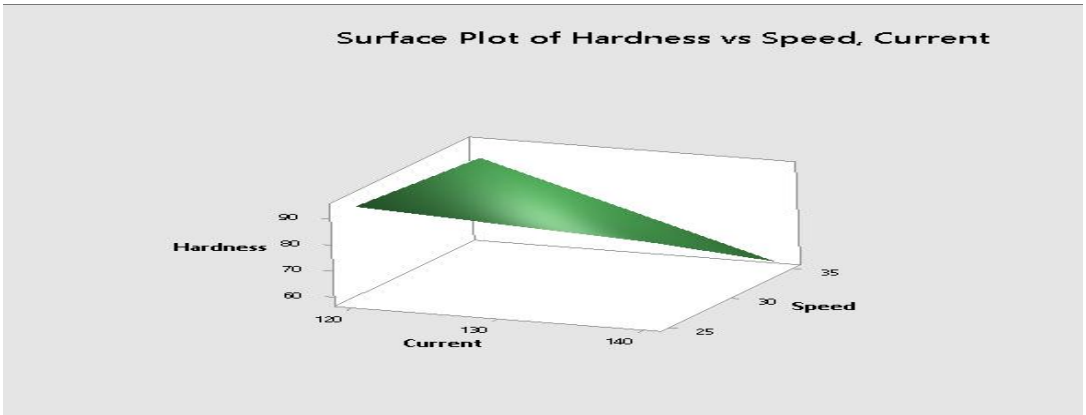


**Figure 6** Interaction plot of speed and current with hardness

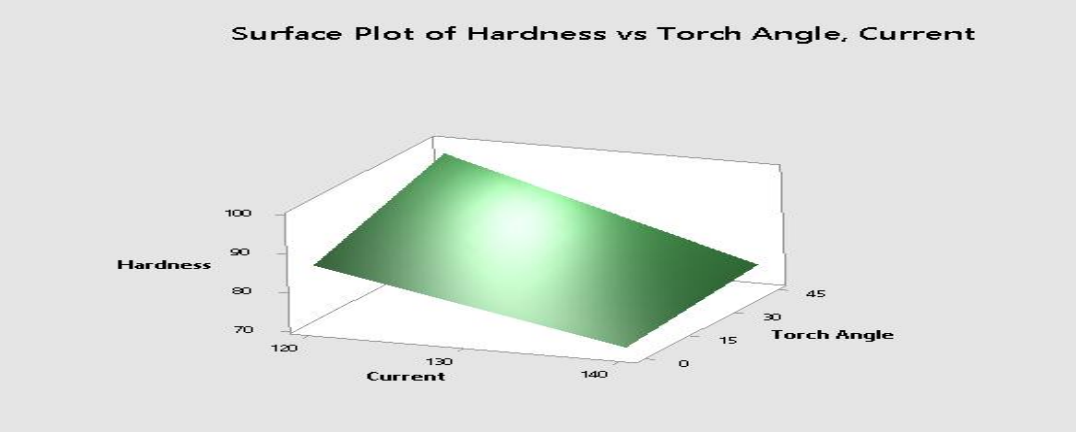


**Figure 7** Interaction plot of torch angle and current with hardness

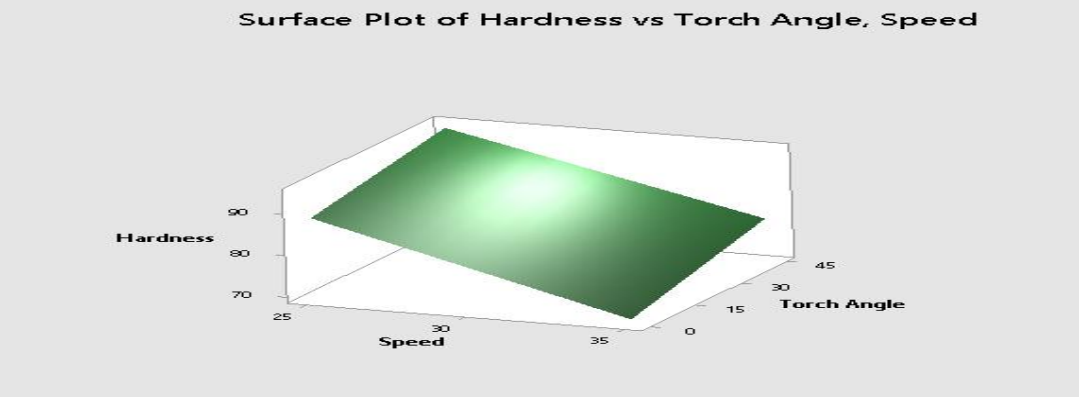


**Figure 8** Interaction plot of torch angle and speed with hardness

## 6.Conclusion

This study is very useful for the industrial application because the fusion of these two metals has better properties against corrosive environment as AISI 304 and AISI 316 contains chromium and nickel. Hardness of the welded joint has a maximum value at

the weld zone. It is clear from the study that hardness of these two materials after fusion will increase and maximum hardness can be achieved with the combination torch angle and the welding speed. The approximate value of BHN at this combination is 80. An increase in current will decrease the hardness. So, for the better result current has to kept minimum and the torch angle must also be minimized. Higher hardness, HRB 80 can be achieved at 120 Amp current and $0^0$ Torch angle. In case of interaction of welding speed and torch angle, best result of hardness can be achieved at a minimum welding speed and maximum torch angle.

## Acknowledgment
None.

## Conflicts of interest
The authors have no conflicts of interest to declare.

## Author's contribution statement
**Deeksha Narwariya:** Conceptualization, investigation, data curation, writing-original draft. **Aditya Kumar Rathi:** conceptualization, writing-draft correction, analysis and interpretation of results, writing-review and editing, writing-conclusion.

## References
[1] Fei Z, Pan Z, Cuiuri D, Li H, Wu B, Ding D, et al. Effect of heat input on weld formation and tensile properties in keyhole mode TIG welding process. Metals. 2019; 9(12):1-15.
[2] Askeland DR, Fulay PP, Battacharya DK. Essentials of materials science and engineering 2nd ed. S., Australia. 2010.
[3] Jariyaboon M, Davenport AJ, Ambat R, Connolly BJ, Williams SW, Price DA. The effect of welding parameters on the corrosion behaviour of friction stir welded AA2024–T351. Corrosion Science. 2007; 49(2):877-909.
[4] Mvola B, Kah P, Martikainen J. Welding of dissimilar non-ferrous metals by GMAW processes. International Journal of Mechanical and Materials Engineering. 2014; 9(1):1-11.
[5] Devaraj J, Ziout A, Abu QJE. Dissimilar non-ferrous metal welding: an insight on experimental and numerical analysis. Metals. 2021; 11(9):1-31.
[6] Kah P, Shrestha M, Martikainen J. Trends in joining dissimilar metals by welding. In applied mechanics and materials 2014 (pp. 269-76). Trans Tech Publications Ltd.
[7] Shah P, Agrawal C. A review on twin tungsten inert gas welding process accompanied by hot wire pulsed power source. Journal of Welding and Joining. 2019; 37(2):41-51.
[8] Miletić I, Ilić A, Nikolić RR, Ulewicz R, Ivanović L, Sczygiol N. Analysis of selected properties of welded joints of the HSLA steels. Materials. 2020; 13(6):1-25.
[9] Mohyla P, Hajnys J, Sternadelová K, Krejčí L, Pagáč M, Konečná K, et al. Analysis of welded joint properties on an AISI316L stainless steel tube manufactured by SLM technology. Materials. 2020; 13(19):1-14.
[10] Nguyen LT, Hwang JS, Kim MS, Kim JH, Kim SK, Lee JM. Charpy impact properties of hydrogen-exposed 316L stainless steel at ambient and cryogenic temperatures. Metals. 2019; 9(6):1-14.
[11] Gourd LM. Principles of welding technology. London: Edward Arnold; 1986.
[12] Weiss B, Stickler R. Phase instabilities during high temperature exposure of 316 austenitic stainless steel. Metallurgical and Materials Transactions B. 1972; 3(4):851-66.
[13] Li HL, Liu D, Yan YT, Guo N, Feng JC. Microstructural characteristics and mechanical properties of underwater wet flux-cored wire welded 316L stainless steel joints. Journal of Materials Processing Technology. 2016; 238:423-30.
[14] Sharma P, Dwivedi DK. A-TIG welding of dissimilar P92 steel and 304H austenitic stainless steel: mechanisms, microstructure and mechanical properties. Journal of Manufacturing Processes. 2019; 44:166-78.
[15] Sathe SS, Harne MS. Optimization of process parameters in TIG welding of dissimilar metals by using activated flux powder. International Journal of Science and Research. 2013; 4(6):2149-52.
[16] Kulkarni A, Dwivedi DK, Vasudevan M. Dissimilar metal welding of P91 steel-AISI 316L SS with Incoloy 800 and Inconel 600 interlayers by using activated TIG welding process and its effect on the microstructure and mechanical properties. Journal of Materials Processing Technology. 2019; 274(2019):1-14.
[17] Rao VA, Deivanathan R. Experimental investigation for welding aspects of stainless steel 310 for the process of TIG welding. Procedia Engineering. 2014; 97:902-8.
[18] Pasupathy J, Ravisankar V. Parametric optimization of TIG welding parameters using taguchi method for dissimilar joint (Low carbon steel with AA1050). Journal of Scientific & Engineering Research. 2013; 4:25-8.
[19] Badheka VJ, Basu R, Omale J, Szpunar J. Microstructural aspects of TIG and A-TIG welding process of dissimilar steel grades and correlation to mechanical behavior. Transactions of the Indian Institute of Metals. 2016; 69(9):1765-73.
[20] Sathish T, Kumar SD, Muthukumar K, Karthick S. Natural inspiration technique for the parameter optimization of A-GTAW welding of naval steel. Materials Today: Proceedings. 2020; 21:843-6.
[21] Tomaz ID, Colaço FH, Sarfraz S, Pimenov DY, Gupta MK, Pintaude G. Investigations on quality characteristics in gas tungsten arc welding process using artificial neural network integrated with genetic algorithm. The International Journal of Advanced Manufacturing Technology. 2021; 113(11):3569-83.

[22] Mahmood M, Dwivedi VK, Yadav R. Effect of current on the hardness of weld bead generated by TIG welding on mild steel. In advances in industrial and production engineering 2021 (pp. 739-45). Springer, Singapore.
[23] Asibeluo IS, Emifoniye E. Effect of arc welding current on the mechanical properties of A36 carbon steel weld joints. SSRG International Journal of Mechanical Engineering. 2015; 2(9):32-4.
[24] Devanathan C, Shankar E, Sivanand A, Edwin PA. Effect of spindle speed and welding speed on mechanical properties of friction stir welding of AA 6063 with AA 7075. International Journal of Scientific and Technology Research. 2019; 8(10):74-7.
[25] Jassim AK, Ali DC, Laken AH. Effect of metal inert gas welding parameters on the hardness and bending strength of carbon steel plates. In AIP conference proceedings 2021. AIP Publishing LLC.
[26] Bhardwaj B, Singh R, Singh R. To study the effects of welding parameters on MIG welding of stainless steel alloy-202. International Journal of Science Technology & Engineering. 2017; 4(1):132-40.
[27] Huang B, Liu J, Zhang S, Chen Q, Chen L. Effect of post-weld heat treatment on the residual stress and deformation of 20/0Cr18Ni9 dissimilar metal welded joint by experiments and simulations. Journal of Materials Research and Technology. 2020; 9(3):6186-200.
[28] Kulkarni A, Dwivedi DK, Vasudevan M. Microstructure and mechanical properties of A-TIG welded AISI 316L SS-Alloy 800 dissimilar metal joint. Materials Science and Engineering: A. 2020; 790:1-11.
[29] Pahlawan IA, Arifin AA, Marliana E, Irawan H. Effect of welding electrode variation on dissimilar metal weld of 316l stainless steel and steel ST41. In IOP conference series: materials science and engineering 2021 (pp. 1-8). IOP Publishing.
[30] Xu Y, Hou X, Shi Y, Zhang W, Gu Y, Feng C, Volodymyr K. Correlation between the microstructure and corrosion behaviour of copper/316 L stainless-steel dissimilar-metal welded joints. Corrosion Science. 2021; 191:1-12.
[31] Pradhan DK, Sahu B, Bagal DK, Barua A, Jeet S, Pradhan S. Application of progressive hybrid RSM-WASPAS-grey wolf method for parametric optimization of dissimilar metal welded joints in FSSW process. Materials Today: Proceedings. 2022; 50:766-72.
[32] Sun Y, Xue H, Yang F, Wang S, Zhang S, He J, et al. Mechanical properties evaluation and crack propagation behavior in dissimilar metal welded joints of 304 L austenitic stainless steel and SA508 low-alloy steel. Science and Technology of Nuclear Installations. 2022; 2022:1-13.

**Deeksha Narwariya** M.Tech student of NSUT. She presented 3 papers in the international conference during her M.Tech course. Her area of interest is TIG and MIG Welding Processes Applications of Dissimilar Metal Welding. She is presently perusing her research work outside India.
Email: deeksha098@gmail.com

**Aditya Kumar Rathi** obtained his B.E degree from, Karnataka University Dharwad in the year 1993 with Mechanical Engineering. He obtained his Master's degree from Delhi College of Engineering in the year 1999. He joined as Senior Scientific Assistant at Netaji Subhas Institute of Technology in February 1994 and got the promotion as Lectures in year 2002 and subsequently as Assistant Professor in year 2007 and Associate Professor from 2015 onwards, he has a long teaching experience at NSIT about 27 years and published 15 papers in International Journal, 10 papers in International and National Conference. He is a life member of ISTE and IIW. His area of interest is Design and Development of Submerged Arc Welding Fluxes.
Email: aditya.kumar@nsut.ac.in

## Appendix I

| S. No. | Abbreviation | Description |
|---|---|---|
| 1 | AISI | American Iron and Steel Institute |
| 2 | AdjMS | Adjusted Mean Squares |
| 3 | Adj SS | Adjusted Sum of Squares |
| 4 | ANOVA | Analysis of Variance |
| 5 | ANN | Artificial Neural Network |
| 6 | BHN | Brinell Hardness Number |
| 7 | DF | Degree of Freedom |
| 8 | DMW | Dissimilar Metal Welding |
| 9 | FSW | Friction Stir Welding |
| 10 | FSSW | Friction Stir Spot Welding |
| 11 | GA | Genetic Algorithm |
| 12 | GTAW | Gas Tungsten Arc Welding |
| 13 | HAZ | Heat Affected Zone |
| 14 | HRB | Rockwell Hardness at B scale |
| 15 | HSLA | High Strength Low Alloy |
| 16 | MMA | Manual Metal Arc |
| 17 | MAG | Metal Active Gas |
| 18 | MIG | Metal Inert Gas |
| 19 | RSM | Response Surface Methodology |
| 20 | SEM | Scanning Electron Microscope |
| 21 | SLM | Selective Laser Melting |
| 22 | SWAW | Shielded Metal Arc Welding |
| 23 | $TiO_2$ | Titanium Die Oxide |
| 24 | TIG | Tungsten Inert Gas |
| 25 | TTP | Temperature Time Precipitation |
| 26 | V-I | Voltage and Current |
| 27 | 3D | Three Dimensional |